RESEARCH PAPER

# Regulation of $I_{Ca,L}$ and force by PDEs in human-induced pluripotent stem cell-derived cardiomyocytes

Umber Saleem[1,4]  |  Djemail Ismaili[1,2,4]  |  Ingra Mannhardt[1,4]  |
Hans Pinnschmidt[3]  |  Thomas Schulze[1,4]  |  Torsten Christ[1,4]  |
Thomas Eschenhagen[1,4]  |  Arne Hansen[1,4]

[1]Department of Experimental Pharmacology and Toxicology, University Medical Center Hamburg-Eppendorf, Hamburg, Germany

[2]Department of Cardiology-Electrophysiology, University Heart Center, University Medical Center Hamburg-Eppendorf, Hamburg, Germany

[3]Department of Medical Biometry and Epidemiology, University Medical Center Hamburg-Eppendorf, Hamburg, Germany

[4]German Center for Heart Research (DZHK), Hamburg, Germany

**Correspondence**
Arne Hansen, Department of Experimental Pharmacology and Toxicology, University Medical Center Hamburg-Eppendorf, Hamburg, Germany.
Email: ar.hansen@uke.de

**Background and Purpose:** Phosphodiesterases (PDEs) are important regulators of β-adrenoceptor signalling in the heart. While PDE4 is the most important isoform that regulates $I_{Ca,L}$ and force in rodent cardiomyocytes, the dominant isoform in adult human cardiomyocytes is PDE3.

**Experimental Approach:** Given the potential of human-induced pluripotent stem cell-derived cardiomyocytes (hiPSC-CMs) for biomedical research, this study characterized the contribution of PDE3 and PDE4 isoforms to the regulation of $I_{Ca,L}$ and force in hiPSC-CMs in an engineered heart tissue (EHT) model.

**Key Results:** There was a lower abundance of mRNA for PDE3A and 4A in hiPSC-CM EHT than in non-failing human heart samples. Selective inhibition of PDE3 and 4 with cilostamide and rolipram, respectively, showed that, in hiPSC-CM, PDE4 was the predominant isoform for the regulation of $I_{Ca,L}$ (cilostamide: +1.44-fold; rolipram: +1.77-fold). Furthermore, in contrast to cilostamide, rolipram decreased the $EC_{50}$ of isoprenaline about 15-fold.

**Conclusion and implications:** The predominance of PDE4 over PDE3 is a peculiarity of hiPSC-CMs and is probably an indicator of immaturity. This finding has implications for the use of hiPSC-CM as pharmacological models to investigate and assess the effects of PDE inhibitors.

# 1 | INTRODUCTION

The phosphodiesterases (PDEs), as designated by the International Union of Pharmacology, hydrolyse cyclic nucleotides. Thus, they regulate a multitude of biological functions in numerous cell types by modulating the concentration of the second messengers cAMP and cGMP. Eleven PDE families have been identified with different substrate selectivity and sensitivity to calcium–calmodulin. The selectivity of PDEs for different processes is achieved through their localization in intracellular compartments and signalosomes (Maurice et al., 2014).

In cardiomyocytes, PDE activity restricts spatiotemporally the effects of β-adrenoceptor stimulation. Accordingly, PDE inhibitors increase the sensitivity of cardiomyocytes to β-adrenoceptor agonists. By mRNA and protein analysis and functional measurements, PDE3 and PDE4 have been identified as the major contributors to PDE activity in rodent cardiomyocytes (Johnson, Katugampola, Able, Napier, & Harding, 2012). Important differences in PDE expression have been shown between rodent and human hearts. In rodent hearts, PDE4D makes up the majority of all PDE activity with a small contribution from PDE4A and PDE4B. In human hearts, the activity of PDE4 is similar to rodents, but it contributes only 8% of all PDE activity because, in human cardiomyocytes, other PDE isoforms (in particular PDE3) are substantial contributors (Richter et al., 2011).

Accordingly, selective inhibition of PDE3 increased $I_{Ca,L}$ and force in human atrial trabeculae by about 20% above baseline, while inhibition of PDE4 by rolipram was without effect (Berk et al., 2016). In human ventricular trabeculae, cilostamide and rolipram alone had no effect on force and relaxation (Molenaar et al., 2013). In the same model, positive inotropic and lusitropic effects mediated by β1- and β2-adrenoceptors were potentiated by cilostamide but not by rolipram. In line with this, Molina et al. demonstrated an increase in $I_{Ca,L}$ and force in un-stimulated human atrial myocytes by selective PDE3 inhibition with cilostamide, while selective PDE4 inhibition with rolipram induced only a minor increase in $I_{Ca,L}$ and no increase in force (Molina et al., 2012). These findings indicate that PDE3 is the dominant isoform in human cardiac tissue and PDE4 the dominant isoform in rodent hearts (Eschenhagen, 2013).

Engineered heart tissue derived from human-induced pluripotent stem cell cardiomyocytes (hiPSC-CM EHT) is a three-dimensional, force-developing, heart muscle model, consisting of hiPSC-CM in a fibrin hydrogel suspended between two flexible silicone posts. Compared to a two-dimensional (2D) culture format, hiPSC-CM in EHTs display morphological, metabolic, and electrophysiological features of improved maturation (Lemoine et al., 2017; Mannhardt et al., 2016; Ulmer et al., 2018; Uzun et al., 2016). In the course of a blinded analysis of 10 compounds, rolipram showed a positive lusitropic and inotropic effect in contrast to milrinone, suggesting a predominance of PDE4 over PDE3 in this model (Mannhardt et al., 2017). To unravel this apparent difference from adult human heart preparations, we analysed PDE isoform expression by quantitative PCR and performed functional analysis of PDE responses in hiPSC-CM EHTs.

**What is already known**
- PDEs regulate β-adrenoceptor signalling in the heart.
- PDE3 is the predominant isoform in adult human cardiomyocytes.

**What this study adds**
- Relevance of PDE3 and PDE4 was assessed in human-induced pluripotent stem cell-cardiomyocytes (hiPSC-CMs).
- PDE4 was the predominant isoform for the regulation of $I_{Ca,L}$ and force in hiPSC-CM.

**What is the clinical significance**
- The predominance of PDE4 over PDE3 is a peculiarity of hiPSC-CMs.
- This finding has implications in the use of hiPSC-CM to analyse inotropic effects.

# 2 | METHODS

## 2.1 | Human tissue samples

For the PCR assays (see below, section 2.3), myocardial tissue was obtained from patients undergoing cardiac surgery at the University Heart Center, Hamburg. The study followed the declaration of Helsinki (Local Ethics Committee approval number PV3759). All patients gave written informed consent. Patient characteristics are given in Table S2. For the measurements of calcium current by patch clamp (section 2.4), adult myocardial tissue was obtained with informed consent from patients undergoing heart transplantation at the Department of Heart Surgery, Dresden University of Technology. Tissue was taken from the free left lateral wall near the mitral valve. These studies were approved by the Medical Faculty Ethics Committee of Dresden University of Technology (document EK790799).

## 2.2 | Expansion and differentiation of human-induced pluripotent stem cells, generation of engineered heart tissue

Experiments were performed as recently described (Breckwoldt et al., 2017; Mannhardt et al., 2016). In brief, human-induced pluripotent stem cells were expanded on geltrex-coated cell culture vessels with FTDA medium (containing bFGF, TGF-β1, dorsomorphin, and activin A) and split with EDTA (0.5 mM; 10 min). Formation of embryoid bodies was achieved in spinner flasks, and differentiation was conducted in cell culture vessels coated for suspension culture (1-mM Pluronic F127) with sequential administration of growth factor- and

small molecule-based cocktails to induce mesodermal progenitors, cardiac progenitors, and cardiomyocytes. Dissociation of differentiated cardiomyocytes was performed with collagenase (0.08%), and dissociated cardiomyocytes were analysed for cardiac differentiation efficiency (FACS for cardiac troponin T) and subjected to EHT generation (Breckwoldt et al., 2017; Mannhardt et al., 2016). Agarose casting moulds were generated in 24-well plates with Teflon spacers (EHT Technologies). Polydimethylsiloxane (PDMS) racks (EHT Technologies) were placed on the 24-well plates so that pairs of PDMS posts reached into the agarose casting moulds. Dis-associated hiPSC-CMs were resuspended in a fibrinogen (final concentration: 5 mg·ml$^{-1}$) reconstitution mix. For each EHT, 97 μl of this mix was briefly mixed with 3-μl thrombin and pipetted into the agarose casting mould. After fibrin polymerization (2 hr), PDMS racks with fibrin gel blocks attached to the PDMS posts were transferred to new 24-well plates. Under cell culture conditions (cell culture media: DMEM, 1% penicillin/streptomycin, 10% horse serum, 10 mg·ml$^{-1}$ insulin, and 33 mg·ml$^{-1}$ aprotinin; incubator condition: 7% $CO_2$ and 40% $O_2$), strip-format, force-generating EHTs attached to PDMS posts developed within 15–20 days.

## 2.3 | PCR

RNA was isolated, from samples of human myocardial tissue, by RNeasy mini kit according to the manufacturer's instructions (Qiagen). Reverse transcription was performed by high-capacity cDNA reverse transcription kit according to manufacturer's instruction (Applied Biosystem). Controls without reverse transcription (−RT) served as negative controls. PCR primers are listed in Table S1. Quantitative PCR was done on the AbiPrism 7900HT Fast Real-Time PCR System (Applied Biosystems) with SYBR Green (Fermentas) according to the manufacturer's instructions in technical triplicates. Values represent the mean of biological and technical triplicates. Glucoronidase beta (identifier: P08236.2) was used as a housekeeping gene (GUSB_for: 5′-AAACGATTGCAGGGTTTCAC-3′; GUSB_rev: 5′-CTCTCGTCGGTGACTGTTCA-3′).

## 2.4 | Measurement of calcium current

Patch clamp experiments, using human adult myocardial tissue, were performed at the Department of Experimental Pharmacology and Toxicology, Medical Faculty, Dresden University of Technology, between 2006 and 2011. The tissue was cut into small pieces in $Ca^{2+}$-free isolation buffer of the following composition (in mM): NaCl 100, KCl 10, $KH_2PO_4$ 1.2, $MgSO_4$ 5, MOPS 5, glucose 20, taurine 50 (pH 7.0), and washed three times for 3 min. During the complete isolation procedure, the solutions were oxygenated with 100% $O_2$ at 37°C. For enzymic dissociation of the tissue pieces, 246 U·ml$^{-1}$ collagenase type I (Worthington Biochemical Corp., NJ, USA) and 0.5 mg·ml$^{-1}$ protease type XXIV (Sigma-Aldrich Co., St Louis, USA) were added to the nominally $Ca^{2+}$-free buffer. After gentle stirring for 10 min, 0.2-mM $Ca^{2+}$

was added, and the tissue was stirred for another 35 min. Solution was changed, and the digestion was continued with 246 U·ml$^{-1}$ collagenase type I in the presence of 0.2-mM $Ca^{2+}$. Stirring of the solution containing the tissue fragments was stopped when single rod-shaped, striated myocytes could be detected in test droplets under the microscope. The suspension was centrifuged, and myocytes were resuspended and stored until use in Tyrode's solution (supplemented with 0.5-mM $Ca^{2+}$ in three steps) at room temperature. One drop of a suspension containing freshly isolated left ventricular (LV) cells was transferred to a patch clamp recording chamber. LV cells settled down within 5 min and remained fixed even when the chamber was perfused. HiPSC-CMs from EHTs were isolated with 200 U·ml$^{-1}$ collagenase type II (Worthington Biochemical Corp., NJ, USA) for 5 hr. In order to support dissociation, trituration was performed after 1.5 and 3 hr, respectively. In contrast to LV cells, EHT cells do not fix on the bottom of a recording chamber. Therefore, EHT cells had to be plated on gelatin-coated (0.1%) glass coverslips and kept in culture for 24 hr. Cover slips with EHT cells were then transferred to the recording chamber. $I_{Ca,L}$ was measured at 37°C using the whole-cell configuration of the patch-clamp technique (Axopatch 200B, Axon Instruments, Foster City, CA, USA), and ISO2 software was used for data acquisition and analysis (MFK, Niedernhausen, Germany). Heat-polished pipettes were pulled from borosilicate filamented glass (Hilgenberg, Malsfeld, Germany). Tip resistances were 2.5–5 MΩ, and seal resistances were 3–6 GΩ. Capacitance ($C_m$) was calculated from the rate and amplitude changes in the voltage responses under voltage clamp from −40 to −35 mV using an algorithm implemented in the abovementioned ISO2 software. $Ca^{2+}$ currents were elicited by applying test pulses from −80 to +10 mV (0.5 Hz, 200-ms pulse duration). $Ca^{2+}$ current amplitude was determined as the difference between peak inward current and current at the end of the depolarizing step and expressed as current density. The cells were investigated in a small perfusion chamber placed on the stage of an inverted microscope. Drugs were applied with a system for rapid solution changes (Cell Micro Controls, Virginia Beach, VA, USA; ALA Scientific Instruments, Long Island, NY, USA). In order to avoid contaminating currents, $K^+$ currents were blocked by replacing $K^+$ with $Cs^+$ and tetraethylammonium-chloride in the bath solution. The experiments were performed with the following $Na^+$-free bath solution (in mM): tetraethylammonium chloride 120, CsCl 10, HEPES 10, $CaCl_2$ 2, $MgCl_2$ 1, and glucose 20 (pH 7.4, adjusted with CsOH). The pipette solution (pH 7.2, adjusted with CsOH) included (in mM) the following: caesium methanesulfonate 90, CsCl 20, HEPES 10, Mg-ATP 4, Tris-GTP 0.4, EGTA 10, and $CaCl_2$ 3 (Christ et al., 2001). In patch clamp experiments, cells were exposed to PDE inhibitors and isoprenaline/norepinephrine for 2 min according to an established protocol (Christ, Molenaar, Klenowski, Ravens, & Kaumann, 2011).

## 2.5 | Measurement of contractile force

Force was analysed by video-optical recording (Hansen et al., 2010; Schaaf et al., 2011). In brief, EHTs in 24-well format were placed in

the incubator chamber of a video-optical contractility test system (EHT Technologies). XYZ camera coordinates were defined for each EHT on the 24-well plate. Software-based automated video-optical recording of EHT contractility was started. Video files were generated and analysed by automated identification of top and bottom ends of the EHT contour. Force was calculated based on EHT shortening and the elastic propensity and geometry of the PDMS posts to which the EHTs were attached. Force/time diagrams were generated automatically, and average values for force and parameters of kinetics were calculated. This procedure was performed at baseline and after compound incubation. HiPSC-CM EHTs were incubated with PDE inhibitors for 30 min and isoprenaline for 20 min in 24-well plates in Tyrode's solution with submaximal calcium, and isoprenaline concentration response curves were performed. For the analysis, only contraction recordings were considered, in which the contractions followed the pacing frequency. Recordings in which the EHTs were beating at a higher frequency than the pacing signal were excluded from the analysis.

## 2.6 | Data and statistical analysis

The data and statistical analysis comply with the recommendations of the *British Journal of Pharmacology* on experimental design and analysis in pharmacology (Curtis et al., 2018). Sample size (power analysis) was planned based on our prior studies for isoprenaline (Mannhardt

et al., 2016). We aimed for $n = 6$ EHTs +50% safety margin per experimental condition according to *BJP* guidelines (McGrath, McLachlan, & Zeller, 2015). As a result, experimental groups were equal in size. Assignment to experimental groups was done by drawing lots for calcium current measurement presented in Figure 2. For contractility analysis presented in Figures 3, 4, and 5, EHTs were randomly assigned to time-matched control, vehicle control and PDE inhibitor groups. Blinding was not undertaken for experiments, but data analysis for Figure 2 was performed under blinded conditions by two independent researchers. For contractility data (Figures 3, 4, and 5), EHTs were analysed by an automated unbiased video optical analysis system which calculates force, frequency, and parameters of kinetics and summarize it in PDF reports.

Statistical analyses were performed with GraphPad Prism (software 5.0), RRID: SCR_002798 (link) and with SPSS version 25.0 (IBM Corp., Armonk, NY), RRID: SCR_002865 (link). By standard qPCR data (Figure 1) were presented relative to house-keeping gene expression. For data in Figures 2, 3, and 5, histograms of data distributions of dependent variables were visually examined, and variances across categories of grouping variables were computed and assessed for homogeneity. For data presented in Figures 2 and 3, the values of the dependent variable were transformed to their natural logarithm because they were right-skewed. Linear mixed-effects models were fitted to the data (SPSS routine GENLINMIXED). Two separate models were fitted to the LV and EHT data for Figure 2, with conditions (time-matched control, TMC; cilostamide, Cil; rolipram, Rol;
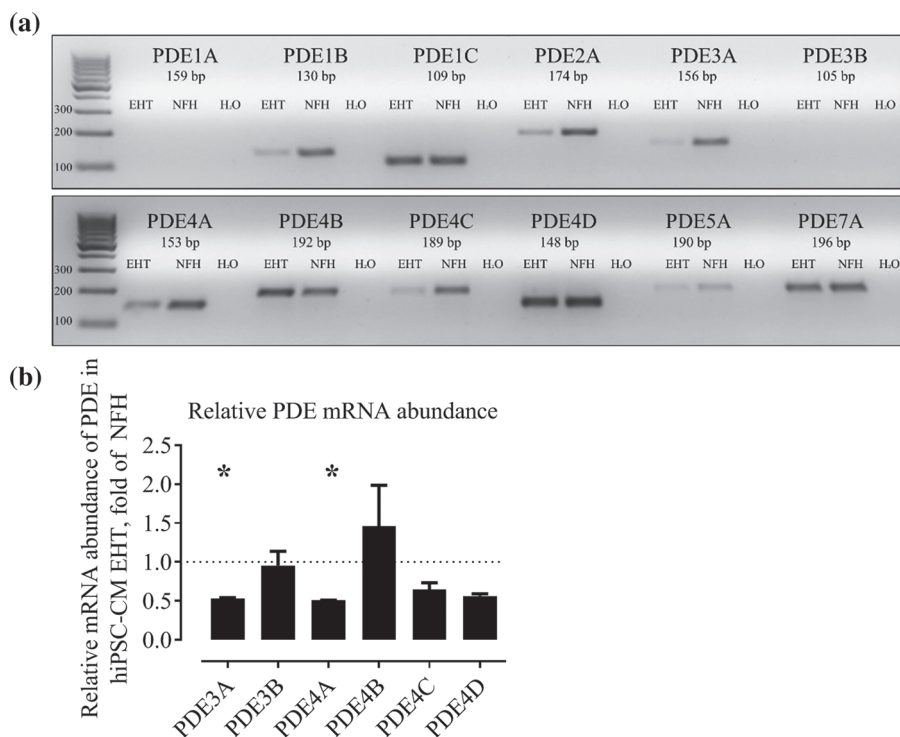


**FIGURE 1** (a) Qualitative RT-PCR of different PDE-isoforms (35 cycles). NFH: non-failing heart. (b) Quantitative RT-PCR. Relative mRNA abundance of PDE3 and 4 isoforms in hiPSC-CM EHTs, normalized to NFH, mean ± *SEM*, $n = 5$ for NFH and hiPSC-CM EHTs (ΔΔCT). $P < .05$, significantly different from NFH samples; $t$ test for unpaired samples. Note, higher sensitivity allowed detection of PDE3B in quantitative PCR (Figure 1b) but not in qualitative PCR (Figure 1a). This figure is related to Figure S1
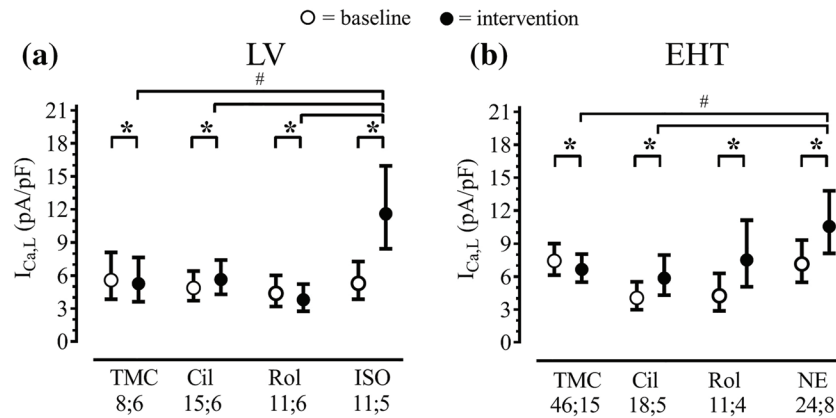
○ = baseline    ● = intervention



**FIGURE 2** Effect of PDE-inhibitors and β-adrenoceptor agonists on calcium current in myocytes from human LV (a) and hiPSC-EHTs (b). Baseline and intervention, model-estimated marginal means with 95% confidence intervals after back-transformation (exponentiation), $P < .05$, significantly different as indicated, baseline versus respective intervention, $^{\#}P < .05$, significantly different as indicated between interventions; pairwise comparisons sequentially step-down rejective Bonferroni-adjusted; $n$; $n$ = number of cells; number of patients, or number of EHTs; number of differentiation batches. TMC: time control; Cil: cilostamide (0.3 μM); Rol: rolipram (10 μM); ISO: isoprenaline (10 μM), NE: noradrenaline (100 μM). Results of $F$ tests for LV ($F$ values with dfmean;dferror in brackets) with $P$ values of effects: $P_{condition\ (TMC,\ Cil,\ Rol,\ ISO)} = .039$ ($F[3;41] = 3.045$), $P_{time\ point\ (baseline,\ intervention)} < .001$ ($F[1;41] = 27.41$), $P_{Condition \times Time\ point} < .001$ ($F[3;41] = 36.50$). Results of $F$ tests for EHT ($F$ values with dfmean;dferror in brackets) with $P$ values of effects: $P_{condition\ (TMC,\ Cil,\ Rol,\ NE)} = .029$ ($F[3;95] = 3.137$), $P_{time\ point\ (baseline,\ intervention)} < .001$ ($F[1;95] = 90.81$), $P_{Condition \times Time\ point} < .001$ ($F[3;95] = 31.24$). See Section 2 for further information on data analytical procedures. This figure is related to Figure S3
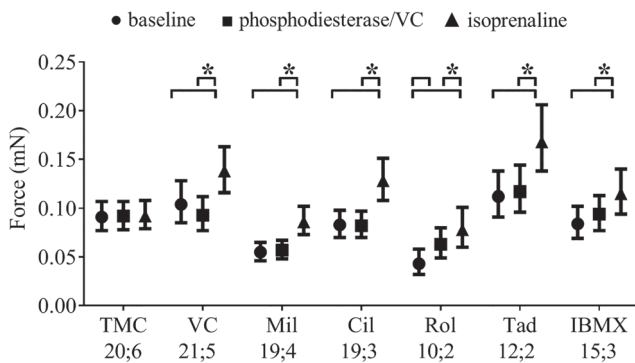


**FIGURE 3** Effect of PDE inhibitors on force and on isoprenaline response (10 nM) in electrically stimulated (1.5–2.0 Hz) hiPSC-EHTs. Graph shows model-estimated marginal means at baseline, PDE/VC and isoprenaline, with 95% confidence intervals after back-transformation (exponentiation); $P < .05$, significantly different as indicated; pairwise comparisons (sequentially step-down rejective Bonferroni-adjusted), between conditions indicated by brackets. TMC: time control ($n = 20$; 6); VC: vehicle control, DMSO 0.1% ($n = 21$; 5); Mil: milrinone (10 μM, $n = 19$; 4); Cil: cilostamide (300 nM, $n = 19$; 3); Rol: rolipram (10 μM, $n = 10$; 2); Tad: tadalafil (10 nM, $n = 12$; 2); IBMX (10 μM, $n = 15$; 3), $n$; $n$ = number of EHTs; number of differentiation batches: the number of EHTs was used for statistics. Results of $F$ tests ($F$ values with dfmean;dferror in brackets) with $P$ values of effects: $P_{condition\ (TMC,\ VC,\ Mil,\ Cil,\ Rol,\ Tad,\ IBMX)} < .001$ ($F[6;115] = 8.354$), $P_{time\ point\ (BL,\ PDE,\ ISO)} < .001$ ($F[2;221] = 130.2$), $P_{Condition \times Time\ point} < .001$ ($F[12;\ 221] = 16.21$). $F$ test results were calculated from the adjusted data set. See Section 2 for further information on data analytical procedures. This figure is related to Figure S2

noradrenaline /isoprenaline: NE/ISO) and time points (baseline, intervention) as fixed effects. Fixed effects for Figure 3 data were also conditions (TMC, vehicle control: VC, Mil, Cil, Rol, Tad, IBMX) and

time points (baseline, PDEI, isoprenaline) while for Figure 5 data, the fixed effect was condition (VC, Mil, Cil, Rol, Tad, IBMX). Interaction terms for Condition × Time point were also included in the models. Random intercepts were assumed for replicates and time points within a measurement, except for Figure 5 data where only one observation per cell was available. The Satterthwaite method to determine the degrees of freedom was employed. For Figure 3 and Figure 5 data, regression weights sensu (Neter, Kutner, Nachtsheim, & Wasserman, 1996) were used to account for variance heterogeneity. Model-estimated marginal means and their 95% confidence intervals were computed, and multiple group comparisons were done by pairwise contrasts subjected to a sequentially step-down rejective Bonferroni procedure to control the α error for multiple testing. Replicate number information is provided both on the number of cells and preparations and expressed as "number of EHTs; hiPSC-CM differentiation batches", or "LV cells; patient samples". All statistical tests were performed based on the number of EHTs or LV cells. A $P$ value < .05 was considered significant. When more than one cell from a patient was available for one experimental group, mean values were calculated for individual patients.

## 2.7 | Materials

The suppliers of the materials used in these experiments are as follows: Sigma-Aldrich supplied **isoprenaline** (I6504); noradrenaline (A7257); milrinone (M4659); tadalfil (Y0001417); Pluronic F127, (P2443); fibrinogen, (F8630); insulin, (I9278); aprotinin, (A1153). R&D Systems supplied cilostamide (091510) and rolipram (90510) and Gibco supplied penicillin/streptomycin (15140) and Geltrex
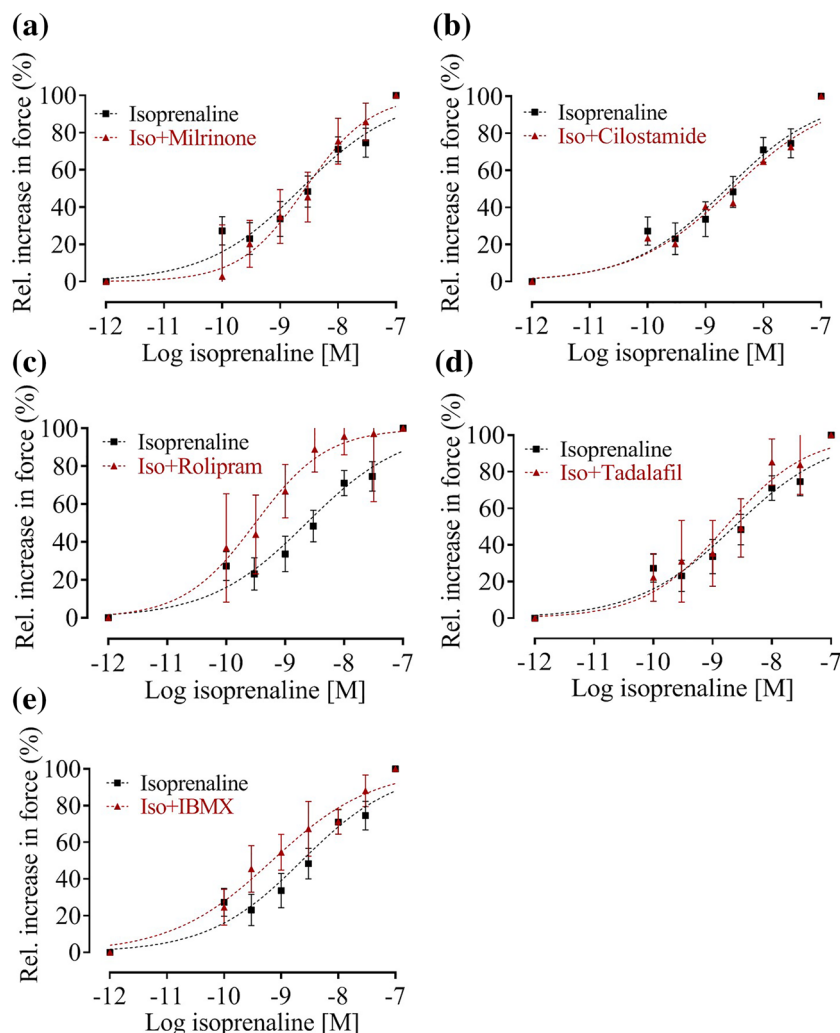
**FIGURE 4** Effect of PDE inhibitors on the potency of isoprenaline to induce positive inotropy in hiPSC-CM EHTs. Mean with 95% confidence interval of normalized force data. Nonlinear regression curve fit with variable Hill slope. Vehicle: DMSO 0.1% (n = 45; 6); Mil: milrinone (10 μM, n = 17; 3); Cil: cilostamide (300 nM, n = 22; 3); Rol: rolipram (10 μM, n = 10; 2); Tad: tadalafil (10 nM, n = 10; 2); IBMX (10 μM, n = 15; 3), n; n = number of EHTs; number of differentiation batches, the number of EHTs was used for statistics. Curve fitting was performed with GraphPad Prism software 5.0. Two constrains (lowest value = 0, highest value = 100) were applied. P < .05, significantly different as indicated

(A1413302). Other sources of compounds were: EDTA: Roth (8043.2); collagenase II, Worthington (LS004176); anti-cardiac troponin T-FITC, recombinant human IgG1, clone REA400, 1:10, Miltenyi Biotec (130–106-687); agarose, Invitrogen (15510–027); thrombin, Peprotech (100–21); horse serum, Life technologies (26050088); DMEM, Biochrom (F0415).

## 2.8 | Nomenclature of targets and ligands

Key protein targets and ligands in this article are hyperlinked to corresponding entries in https://www.guidetopharmacology.org, the common portal for data from the IUPHAR/BPS Guide to Pharmacology (Harding et al., 2018), and are permanently archived in the Concise Guide to Pharmacology 2019/2020 (Alexander, Christopoulos et al., 2019; Alexander, Fabbro et al., 2019).

## 3 | RESULTS

### 3.1 | Expression of PDE in hiPSC-CM EHTs and non-failing heart

PCR primers were designed to determine mRNA abundance of the following PDE isoforms and family members: PDE1A/B/C, PDE2A, PDE3A/B (Zhao et al., 2019), PDE4A/B/C/D, **PDE5A**, and PDE7A. Qualitative RT-PCR was performed on total RNA of hiPSC-CM EHTs and samples of human non-failing hearts (Figure 1a). PDE isoforms 1B, 1C, 2A, 3A, 4A, 4B, 4C, 4D, and 7A gave robust signals in both samples. In contrast, only a faint band was detected for PDE5A, whereas PDE1A and 3B could not be amplified in both samples. The direct comparison between hiPSC-CM and non-failing heart tissue revealed a stronger band in non-failing heart for PDE1B, 2A, 3A, 4A, and 4C (Figure 1a). Quantitative PCR was performed for PDE3 and
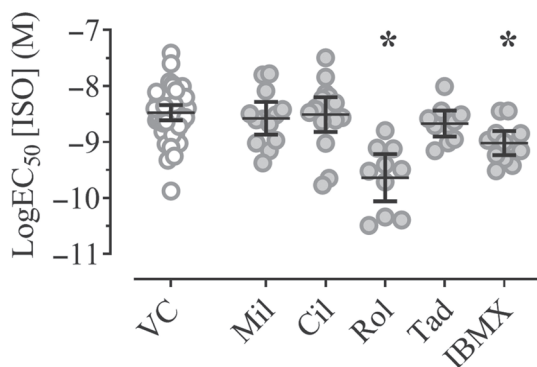
**FIGURE 5** Effect of PDE inhibitors on the inotropic potency of isoprenaline in electrically stimulated (1.5–2.0 Hz) hiPSC-CM EHTs, expressed as LogEC$_{50}$ for isoprenaline of data shown in Figure 4. Scatter plot of raw data with mixed model-estimated marginal means and 95% confidence intervals; $P < .05$, significantly different from vehicle control (VC); pairwise comparisons (sequentially step-down rejective Bonferroni-adjusted). VC: DMSO 0.1%, $n = 45; 6$); Mil: milrinone (10 μM, $n = 17; 3$); Cil: cilostamide (300 nM, $n = 22; 3$); Rol: rolipram (10 μM, $n = 10; 2$); Tad: tadalafil (10 nM, $n = 10; 2$); IBMX (10 μM, $n = 15; 3$), $n$; $n$ = number of EHTs; number of differentiation batches, the number of EHTs were used for statistics. $F$ test results ($F$ values with dfmean;dferror in brackets) with $P$ value for the effect of condition: $P_{condition (VC, Mil, Cil, Rol, Tad, IBMX)} < .001$ ($F[5;113] = 9.744$). $F$ test results were calculated from the adjusted data set. See Section 2 for further information on data analytical procedures

PDE4 isoforms in hiPSC-CM EHTs and non-failing heart samples and showed a significant (0.5-fold) lower expression of PDE3A and 4A transcripts in hiPSC-CM relative to that in non-failing heart tissue (Figure 1b). Estimation of absolute expression level by raw cycle threshold values (CT, Figure S1) suggested that in non-failing heart tissue, **PDE3A** (mean CT: 24.8), PDE4D (mean CT: 25.6) and PDE4A (mean CT: 25.8) were expressed at high level and PDE3A (mean CT: 27.7), PDE4D (mean CT: 27.6), and PDE4B (mean CT: 27.8) were expressed at high level in hiPSC-CM EHTs.

## 3.2 | EFFECTS OF PDE INHIBITORS ON I$_{CA,L}$

In LV myocytes, I$_{Ca,L}$ current density was between 4.4 and 5.6 pA·pF$^{-1}$ (minimum–maximum mean values, Figure 2a) at baseline. I$_{Ca,L}$ increased in the presence of cilostamide by 16%. Rolipram decreased I$_{Ca,L}$ similar to the time-matched control suggesting that this is due to experimental run down and does not reflect a compound effect. The increase in I$_{Ca,L}$ by a maximally effective concentration of isoprenaline (10 μM) was 119%. Comparison of ΔI$_{Ca,L}$ between interventions revealed a significantly higher value for isoprenaline compared with cilostamide, rolipram, and time-matched control (Figure 2a). In hiPSC-CM from EHTs, I$_{Ca,L}$ current density was between 4.1 and 7.4 pA·pF$^{-1}$ (minimum–maximum mean values, Figure 2b) at baseline. As in LV, cilostamide slightly increased I$_{Ca,L}$ in hiPSC-CM EHTs by 44%. In contrast to LV, rolipram and noradrenaline evoked a strong increase in I$_{Ca,L}$ (77% and 48%, respectively). Comparison of ΔI$_{Ca,L}$ between

interventions revealed a significantly higher value for noradrenaline, compared with cilostamide and time-matched control but not to rolipram (Figure 2b). Original sample traces are displayed in Figure S3, and model-estimated marginal means, confidence intervals, and pairwise contrast data are shown in Tables S3, S4, and S5.

## 3.3 | Effects of PDE inhibitors on force

The increase in I$_{Ca,L}$ by PDE inhibitors in hiPSC-CM EHTs led to the question whether PDE inhibitors also increase contractile force. To address this question, force measurements were performed in hiPSC-CM EHTs equilibrated in Tyrode's solution with 0.6-mM Ca$^{2+}$ (~EC$_{50}$) and electrically stimulated at 1.5–2.0 Hz. PDE inhibitors or vehicle and a single submaximal concentration of isoprenaline (100 nM) were added sequentially. Figure 3 demonstrates the effect of PDE inhibitors and isoprenaline on force. Time-matched control and vehicle (0.1% DMSO) control recordings showed no effect on force (Figure 3). Isoprenaline alone increased force by 48%. The PDE3 inhibitor cilostamide (300 nM), milrinone (10 μM), the PDE5 inhibitor tadalafil (10 nM), and the non-selective PDE inhibitor IBMX (10 μM) did not increase force (Figure 3). The PDE4 inhibitor rolipram (10 μM) led to a positive inotropic effect of 46%. Isoprenaline in the presence of PDE inhibitors led to a significant increase in force between 22% and 56% (Figure 3). The Δforce values for isoprenaline effects were independent of baseline force values (Figure S2). Model-estimated marginal means, confidence intervals, and pairwise contrast data are shown in Tables S6 and S7.

## 3.4 | Effects of PDE inhibitors on isoprenaline potency

Concentration–response curves for isoprenaline were performed in hiPSC-CM EHTs in the presence and absence of PDE inhibitors (Figure 4, nonlinear regression curve fit with variable Hill slope). Figure 5 displays the EC$_{50}$ values for this experiment in a scatter plot graph. Model-estimated marginal means, confidence intervals, and pairwise contrast data are shown in Table S8 and S9. The LogEC$_{50}$ of isoprenaline for the force response was −8.52 M (Figures 4 and 5). In the presence of the PDE3 inhibitors, milrinone (10 μM) or cilostamide (300 nM), the potency of isoprenaline remained unchanged. Preincubation with the PDE4 inhibitors rolipram (10 μM) led to a decrease in isoprenaline LogEC$_{50}$ value by 14%. The PDE5 inhibitor tadalafil did not change the isoprenaline LogEC$_{50}$ value. The non-selective PDE inhibitor IBMX led to a decrease in isoprenaline LogEC$_{50}$ value by 8%.

## 4 | DISCUSSION AND CONCLUSIONS

In unstimulated human heart preparations, the non-selective PDE inhibitor IBMX or combined PDE3/4 inhibitors (milrinone, **enoximone**,

and pimobendan) reduced PDE activity and increased contractile force (Bethke et al., 1992; Böhm et al., 1991; Focaccio et al., 1996; Schmitz et al., 1992). In unstimulated human atrial myocytes, selective PDE3 inhibition with cilostamide increased $I_{Ca,L}$ and force, while selective PDE4 inhibition with rolipram induced only a minor increase in $I_{Ca,L}$ and no increase in force (Molina et al., 2012). In unstimulated human LV (myocytes), cilostamide but not rolipram induced a small increase in $I_{Ca,L}$ by 16% (this study, Figure 2a) and neither cilostamide nor rolipram had an effect on force (Molenaar et al., 2013). Collectively, these data point to a major contribution by PDE3 to the regulation of β-adrenoceptor signalling in adult human cardiomyocytes (Eschenhagen, 2013).

Our present data show that hiPSC-CM differ in their regulation by PDE. PDE4 inhibition by rolipram increased basal $I_{Ca,L}$ by 77% and this effect was much larger than that of PDE3 inhibition by cilostamide (44%, Figure 2b). For rolipram. the increase in $I_{Ca,L}$ translated into an increase in force (Figure 3). Consequently, the inotropic potency of isoprenaline was increased by rolipram and by IBMX, but not by cilostamide or milrinone (Figure 5). The results indicate that hiPSC-CM is a cell culture model with strong contribution of PDE to basal and stimulated cAMP regulation and that PDE4 provides the major component of this PDE activity.

This raised the question of whether this predominance of PDE4 over PDE3 was a peculiarity of hiPSC-CM or an indicator of the relative immaturity of these cells. The latter seems to be the case as several studies found evidence for a switch from PDE4 to PDE3 during postnatal heart development in mammals. In rabbits, $I_{Ca,L}$ was found to be regulated predominantly by a rolipram-sensitive PDE in newborn animals, but by a milrinone-sensitive PDE in adults (Akita, Joyner, Lu, Kumar, & Hartzell, 1994). In pig atria, similar changes were reported with regard to regulation of cAMP and force development (Galindo-Tovar, Vargas, Escudero, & Kaumann, 2009).

PDE3 inhibition increased $I_{Ca,L}$ much less than the maximum β-adrenoceptor stimulation, in myocytes from human LV and to a similar extent in hiPSC-CM EHTs (Figure 2). Surprisingly, the effect of PDE4 inhibition in hiPSC-CM EHT was as large as the maximum β-adrenoceptor stimulation, supporting the interpretation of strong control of basal $I_{Ca,L}$ by PDE4. It remains unclear whether this is related to the smaller effect size of β-adrenoceptor stimulation and higher basal cAMP-insensitive $I_{Ca,L}$ in hiPSC-CM EHTs (Uzun et al., 2016).

In LV trabeculae, force was insensitive to selective inhibition of PDE3 or PDE4 by cilostamide or rolipram respectively (Molenaar et al., 2013), while in human atrial myocytes, inhibition of PDE3 by cilostamide evoked an increase in force (Christ, Engel, Ravens, & Kaumann, 2006; Molina et al., 2012). In the rat heart (another pharmacological model dominated by PDE4), force was increased by rolipram in atrial but not in ventricular tissue (Christ, Galindo-Tovar, Thoms, Ravens, & Kaumann, 2009). PDE4 effect size was highest in spontaneous beating right atria (60%), smaller in left atria (40%), and absent in LV (Christ et al., 2009).

In line with the effects of PDE inhibitors on basal $I_{Ca,L}$ and force, the response to catecholamines was regulated only by the PDE4

isoform (Figures 4 and 5). The finding that potentiation by the non-selective PDE inhibitor IBMX was not larger than selective PDE4 inhibition alone, argues against any relevant contribution of other PDE isoforms in hiPSC-CM. In line with this assumption, we found that tadalafil, a selective PDE5 inhibitor did not potentiate the response to isoprenaline. In human and rat LV preparations, potentiation by selective PDE inhibition (cilostamide or rolipram) resulted in a half-log unit shift of the catecholamine concentration–response curve (Christ et al., 2009; Molenaar et al., 2013). As demonstrated in Figure 5, in hiPSC-EHT, the potentiation of catecholamine by rolipram resulted in a one-log unit shift. This result again demonstrates a major contribution of PDE4 to the regulation of cAMP in this model. This finding has implications for the use of hiPSC-CM as a pharmacological model to investigate effects of PDE inhibitors.

Important limitations of this study are as follows: (a) the use of only one hiPSC line and LV from failing hearts and no samples from non-failing hearts, (b) the experimental design to study global cellular PDE expression and not PDE expression in specific compartments/microdomains, and (c) the possibility of contamination of $I_{CaL}$ recordings by the $Na^+/Ca^{2+}$ current due to the absence of $Na^+$ in the extracellular solution.

In summary, this study provides evidence for the restriction of β-adrenoceptor signalling by PDE4 in hiPSC-CM, rather than by PDE3, as in the adult human myocardium.

## AUTHOR CONTRIBUTIONS

T.E., T.C., and A.H. conceived and organized the project and wrote the manuscript; U.S. and D.I. designed and performed the experiments and analysed data with contribution from I.M. and T. S. All authors discussed the results and commented on the manuscript.

## CONFLICT OF INTEREST

T.E., A.H., and I.M. are co-founder of EHT Technologies GmbH.

## DECLARATION OF TRANSPARENCY AND SCIENTIFIC RIGOUR

This Declaration acknowledges that this paper adheres to the principles for transparent reporting and scientific rigour of preclinical research as stated in the *BJP* guidelines for Design & Analysis, and as

recommended by funding agencies, publishers and other organisations engaged with supporting research.

## ORCID

*Umber Saleem* https://orcid.org/0000-0002-0466-3851

## REFERENCES

Akita, T., Joyner, R. W., Lu, C., Kumar, R., & Hartzell, H. C. (1994). Developmental changes in modulation of calcium currents of rabbit ventricular cells by phosphodiesterase inhibitors. *Circulation*, 90, 469–478. https://doi.org/10.1161/01.cir.90.1.469

Alexander, S. P. H., Christopoulos, A., Davenport, A. P., Kelly, E., Mathie, A., Peters, J. A., ... CGTP Collaborators. (2019). The Concise Guide to PHARMACOLOGY 2019/20: G protein-coupled receptors. *British Journal of Pharmacology*, 176, S21–S141. https://doi.org/10.1111/bph.14748

Alexander, S. P. H., Fabbro, D., Kelly, E., Mathie, A., Peters, J. A., Veale, E. L., ... CGTP Collaborators. (2019). The Concise Guide to PHARMACOLOGY 2019/20: Enzymes. *British Journal of Pharmacology*, 176, S297–S396. https://doi.org/10.1111/bph.14752 Berk, E., Christ, T., Schwarz, S., Ravens, U., Knaut, M., & Kaumann, A. J. (2016). In permanent atrial fibrillation, PDE3 reduces force responses to 5-HT, but PDE3 and PDE4 do not cause the blunting of atrial arrhythmias. *British Journal of Pharmacology*, 173, 2478–2489. https://doi.org/10.1111/bph.13525

Bethke, T., Eschenhagen, T., Klimkiewicz, A., Kohl, C., von der Leyen, H., Mehl, H., ... Rosswag, S. (1992). Phosphodiesterase inhibition by enoximone in preparations from nonfailing and failing human hearts. *Arzneimittel-Forschung*, 42(4), 437–445.

Böhm, M., Morano, I., Pieske, B., Rüegg, J. C., Wankerl, M., Zimmermann, R., & Erdmann, E. (1991). Contribution of cAMP-phosphodiesterase inhibition and sensitization of the contractile proteins for calcium to the inotropic effect of pimobendan in the failing human myocardium. *Circulation Research*, 68, 689–701. https://doi.org/10.1161/01.RES.68.3.689

Breckwoldt, K., Letuffe-Brenière, D., Mannhardt, I., Schulze, T., Ulmer, B., Werner, T., ... Hansen, A. (2017). Differentiation of cardiomyocytes and generation of human engineered heart tissue. *Nature Protocols*, 12, 1177–1197. https://doi.org/10.1038/nprot.2017.033

Christ, T., Engel, A., Ravens, U., & Kaumann, A. J. (2006). Cilostamide potentiates more the positive inotropic effects of (–)-adrenaline through β2-adrenoceptors than the effects of (–)-noradrenaline through β1-adrenoceptors in human atrial myocardium. *Naunyn-Schmiedeberg's Archives of Pharmacology*, 374, 249–253. https://doi.org/10.1007/s00210-006-0119-5

Christ, T., Galindo-Tovar, A., Thoms, M., Ravens, U., & Kaumann, A. J. (2009). Inotropy and L-type Ca 2+ current, activated by β 1- and β 2-adrenoceptors, are differently controlled by phosphodiesterases 3 and 4 in rat heart. *British Journal of Pharmacology*, 156, 62–83. https://doi.org/10.1111/j.1476-5381.2008.00015.x

Christ, T., Molenaar, P., Klenowski, P. M., Ravens, U., & Kaumann, A. J. (2011). Human atrial β(1L)-adrenoceptor but not β-adrenoceptor activation increases force and Ca(2+) current at physiological temperature. *British Journal of Pharmacology*, 162, 823–839. https://doi.org/10.1111/j.1476-5381.2010.00996.x

Christ, T., Wettwer, E., Dobrev, D., Adolph, E., Knaut, M., Wallukat, G., & Ravens, U. (2001). Autoantibodies against the β1-adrenoceptor from patients with dilated cardiomyopathy prolong action potential duration and enhance contractility in isolated cardiomyocytes. *Journal of Molecular and Cellular Cardiology*, 33, 1515–1525. https://doi.org/10.1006/jmcc.2001.1414

Curtis, M. J., Alexander, S., Cirino, G., Docherty, J. R., George, C. H., Giembycz, M. A., ... Ahluwalia, A. (2018). Experimental design and analysis and their reporting II: Updated and simplified guidance for authors and peer reviewers. *British Journal of Pharmacology*, 175, 987–993. https://doi.org/10.1111/bph.14153

Eschenhagen, T. (2013). PDE4 in the human heart—Major player or little helper? *British Journal of Pharmacology*, 169, 524–527. https://doi.org/10.1111/bph.12168

Focaccio, A., Peeters, G., Movsesian, M., Roden, R., Eki, Y., Krall, J., & Bristow, M. R. (1996). Mechanism of action of OPC-8490 in human ventricular myocardium. *Circulation*, 93, 817–825. https://doi.org/10.1161/01.cir.93.4.817

Galindo-Tovar, A., Vargas, M. L., Escudero, E., & Kaumann, A. J. (2009). Ontogenic changes of the control by phosphodiesterase-3 and -4 of 5-HT responses in porcine heart and relevance to human atrial 5-HT 4 receptors. *British Journal of Pharmacology*, 156, 237–249. https://doi.org/10.1111/j.1476-5381.2008.00023.x

Hansen, A., Eder, A., Bönstrup, M., Flato, M., Mewe, M., Schaaf, S., ... Eschenhagen, T. (2010). Development of a drug screening platform based on engineered heart tissue. *Circulation Research*, 107, 35–44. https://doi.org/10.1161/CIRCRESAHA.109.211458

Harding, S. D., Sharman, J. L., Faccenda, E., Southan, C., Pawson, A. J., Ireland, S., ... NC-IUPHAR. (2018). The IUPHAR/BPS guide to pharmacology in 2018: Updates and expansion to encompass the new guide to immunopharmacology. *Nucleic Acids Research*, 46, D1091–D1106. https://doi.org/10.1093/nar/gkx1121

Johnson, W. B., Katugampola, S., Able, S., Napier, C., & Harding, S. E. (2012). Profiling of cAMP and cGMP phosphodiesterases in isolated ventricular cardiomyocytes from human hearts: Comparison with rat and guinea pig. *Life Sciences*, 90, 328–336.

Lemoine, M. D., Mannhardt, I., Breckwoldt, K., Prondzynski, M., Flenner, F., Ulmer, B., ... Reichenspurner, H. (2017). Human iPSC-derived cardiomyocytes cultured in 3D engineered heart tissue show physiological upstroke velocity and sodium current density. *Scientific Reports*, 7, 1–11.

Mannhardt, I., Breckwoldt, K., Letuffe-Brenière, D., Schaaf, S., Schulz, H., Neuber, C., ... Hansen, A. (2016). Human engineered heart tissue: Analysis of contractile force. *Stem Cell Reports*, 7, 29–42. https://doi.org/10.1016/j.stemcr.2016.04.011

Mannhardt, I., Eder, A., Dumotier, B., Prondzynski, M., Kr-amer, E., Traebert, M., et al. (2017). Blinded contractility analysis in hipsc-cardiomyocytes in engineered heart tissue format: Comparison with human atrial trabeculae. *Toxicological Sciences*, 158, 164–175. https://doi.org/10.1093/toxsci/kfx081

Maurice, D. H., Ke, H., Ahmad, F., Wang, Y., Chung, J., & Manganiello, V. C. (2014). Advances in targeting cyclic nucleotide phosphodiesterases. *Nature Reviews. Drug Discovery*, 13, 290–314. https://doi.org/10.1038/nrd4228

McGrath, J. C., McLachlan, E. M., & Zeller, R. (2015). Transparency in research involving animals: The Basel declaration and new principles for reporting research in *BJP* manuscripts. *British Journal of Pharmacology*, 172, 2427–2432. https://doi.org/10.1111/bph.12956

Molenaar, P., Christ, T., Hussain, R. I., Engel, A., Berk, E., Gillette, K. T., ... Kaumann, A. J. (2013). PDE3, but not PDE4, reduces ß1- and ß2-adrenoceptor-mediated inotropic and lusitropic effects in failing ventricle from metoprolol-treated patients. *British Journal of Pharmacology*, 169, 528–538. https://doi.org/10.1111/bph.12167

Molina, C. E., Leroy, J., Richter, W., Xie, M., Scheitrum, C., Lee, I. O., ... Fischmeister, R. (2012). Cyclic adenosine monophosphate phosphodiesterase type 4 protects against atrial arrhythmias. *Journal of the American College of Cardiology*, 59, 2182–2190. https://doi.org/10.1016/j.jacc.2012.01.060

Neter, J., Kutner, M.H., Nachtsheim, C.J., and Wasserman, W. (1996). Applied linear statistical models (Irwin).

Richter, W., Xie, M., Scheitrum, C., Krall, J., Movsesian, M. A., & Conti, M. (2011). Conserved expression and functions of PDE4 in rodent and

human heart. *Basic Research in Cardiology*, 106, 249–262. https://doi.org/10.1007/s00395-010-0138-8

Schaaf, S., Shibamiya, A., Mewe, M., Eder, A., Stöhr, A., Hirt, M. N., ... Hansen, A. (2011). Human engineered heart tissue as a versatile tool in basic research and preclinical toxicology. *PLoS ONE*, 6, e26397. https://doi.org/10.1371/journal.pone.0026397

Schmitz, W., Eschenhagen, T., Mende, U., Müller, F. U., Neumann, J., & Scholz, H. (1992). Phosphodiesterase inhibition and positive inotropy in failing human myocardium. *Basic Research in Cardiology*, 87(Suppl 1), 65–71.

Ulmer, B. M., Stoehr, A., Schulze, M. L., Patel, S., Gucek, M., Mannhardt, I., ... Hansen, A. (2018). Contractile work contributes to maturation of energy metabolism in hiPSC-derived cardiomyocytes. *Stem Cell Reports*, 10, 834–847. https://doi.org/10.1016/j.stemcr.2018.01.039

Uzun, A. U., Mannhardt, I., Breckwoldt, K., Horváth, A., Johannsen, S. S., Hansen, A., ... Christ, T. (2016). Ca$^{2+}$-currents in human induced pluripotent stem cell-derived cardiomyocytes effects of two different

culture conditions. *Frontiers in Pharmacology*, 7, 1–14, 300. https://doi.org/10.3389/fphar.2016.00300

Zhao, Y., Rafatian, N., Feric, N. T., Cox, B. J., Aschar-Sobbi, R., Wang, E. Y., et al. (2019). A platform for generation of chamber-specific cardiac tissues and disease modeling. *Cell*, 176, 913–927, e18.

## SUPPORTING INFORMATION

Additional supporting information may be found online in the Supporting Information section at the end of this article.